Tetramethylpyrazine protects retinal ganglion cells against H_2O_2-induced damage via the microRNA-182/mitochondrial pathway

XINMIN LI[1], QIULI WANG[2], YANFAN REN[1], XIAOMIN WANG[1], HUAXU CHENG[1], HUA YANG[1] and BAOJUN WANG[1]

[1]Department of Ophthalmology, The First Affiliated Hospital of Xinxiang Medical University, Weihui, Henan 453100; [2]Department of Ophthalmology, The Third Affiliated Hospital of Xinxiang Medical University, Xinxiang, Henan 453000, P.R. China

Received October 15, 2018; Accepted May 28, 2019

DOI: 10.3892/ijmm.2019.4214

Abstract. Glaucoma is the leading cause of irreversible blindness worldwide; the apoptosis of the retinal ganglion cells (RGCs) is a hallmark of glaucoma. Tetramethylpyrazine (TMP) is the main active component of *Ligusticum wallichii Franchat*, and has been demonstrated to improve a variety of injuries through its antioxidative and antiapoptotic properties. However, these effects of TMP on glaucoma have not been studied. The present study aimed to investigate the potential role of TMP in glaucoma and to elucidate its possible mechanisms responsible for these effects. An *in vitro* model was generated, in which primary RGCs (PRGCs) were treated with H_2O_2. Our study revealed that TMP protected against H_2O_2-induced injury to PRGCs, as evidenced by enhanced cell viability, reduced caspase 3 activity and decreased cell apoptosis. We also reported that TMP treatment inhibited reactive oxygen species (ROS) production and malondialdehyde levels, but upregulated the antioxidative enzyme superoxide dismutase. In particular, TMP significantly increased the expression of microRNA-182-5p (miR-182) in H_2O_2-treated PRGCs, which was selected as the target miRNA for further research. In addition, our findings suggested that the protective effects of TMP on H_2O_2-induced injury were attenuated by knockdown of miR-182. The results of a luciferase reporter assay demonstrated that Bcl-2 interacting protein 3 (BNIP3), an effector of mitochondria-mediated apoptosis, was a direct target of miR-182. In addition, TMP treatment significantly decreased the expression of BNIP3, Bax, cleaved-caspase-3 and cleaved-poly(ADP-ribose)polymerase, but increased that of Bcl-2. Also, TMP treatment decreased the release of cytochrome *c* from mitochondria and improved mitochondrial membrane potential in H_2O_2-treated RGCs. Of note, the inhibitory effects of TMP on the mitochondrial apoptotic pathway were suggested to be reversed by knockdown of miR-182. Collectively, our findings provide novel evidence that TMP protects PRGCs against H_2O_2-induced damage through suppressing apoptosis and oxidative stress via the miR-182/mitochondrial apoptotic pathway.

Correspondence to: Professor Baojun Wang, Department of Ophthalmology, The First Affiliated Hospital of Xinxiang Medical University, 88 Jiankang Road, Weihui, Henan 453100, P.R. China
E-mail: junbaowangjb@163.com

Key words: glaucoma, tetramethylpyrazine, retinal ganglion cells, microRNA-182, mitochondrial apoptotic pathway

Introduction

Glaucoma is a severe eye disease and has been recognized as one of the leading causes of irreversible blindness worldwide (1). Glaucoma has been predicted to affect ~76.0 million people in 2020 globally (2). Despite advancements in the clinical treatment of this disease, few improvements have been made in prognosis. It has been reported that oxidative stress and the apoptosis of retinal ganglion cells (RGCs) are the main hallmarks of the pathogenesis of glaucoma (3-5). Therefore, preventing oxidative stress and apoptosis in RGCs may be an effective therapeutic strategy for treating glaucoma.

Tetramethylpyrazine (TMP), the main active component of *Ligusticum wallichii Franchat*, has been used extensively for the treatment of neurovascular diseases in China for centuries (6,7). As previously reported, TMP possesses therapeutic potential in a variety of diseases by mechanisms mediated by antioxidation and anti-apoptosis (8-10). Additionally, the neuroprotective effects of TMP in retinal diseases have been confirmed *in vitro* and *in vivo* (11,12). For example, Yang *et al* (10) revealed that TMP could preserve neuronal morphology and promote survival in retinal cell cultures, and protected cells against the cytotoxicity of high doses of hydrogen peroxide. Luo *et al* (13) suggested that TMP protects RGCs against N-methyl-D-aspartate-induced excitotoxicity. However, to the best of our knowledge, the effects of TMP on glaucoma remain unknown.

MicroRNAs (miRNAs), a class of endogenous small noncoding RNAs of 18-22 nucleotides, negatively modulate gene expression at the post-transcription level by inhibiting translation or inducing RNA degradation (14,15). Several

studies have demonstrated an important role for miRNAs and their target genes in retinal cell apoptosis (16,17). For example, Li *et al* (18) reported that miR-137 was downregulated under hypoxic conditions and inhibition of miR-137 could protect RGCs against hypoxia-induced apoptosis through targeting the Notch1 pathway. Zhang *et al* (19) revealed that miR-187 inhibited the oxidative stress-induced apoptosis of RGCs by negatively regulating P2X purino receptor 7. Cheng *et al* (20) demonstrated that miR-141 attenuated UV-induced oxidative stress via activating Keap1-Nrf2 signaling in retinal ganglion cells; however, whether TMP exerts its protective effect by regulating miRNA in glaucoma remains unclear.

In the present study, we evaluated the protective effects of TMP against H_2O_2-induced damage in primary RGCs (PRGCs) and an *in vitro* model of oxidative stress injury; the potential role of the miR-182/mitochondrial pathway associated with the neuroprotective effects of TMP was investigated.

Materials and methods

PRGC culture. PRGCs were isolated using Thy1.2-conjugated magnetic beads from the retinas of 20 male BALB/c mice (weighing 20-30 g, 8-weeks old) obtained from the Laboratory Animal Center of The First Affiliated Hospital of Xinxiang Medical University (Xinxiang, China) as previously described (21). All mice were maintained in a temperature-controlled room (22±2˚C) with a 12-h light/dark cycle and a relative humidity of 40-60%, and had free access to food and water. For PRGC culture, tissue culture plates were coated with poly-D-lysine (10 μg/ml; EMD Millipore) and laminin (10 μg/ml; Sigma-Aldrich; Merck KGaA) at 37˚C in a humidified tissue culture incubator with 5% CO_2. Primary cells were identified by immunofluorescence staining with neurofilament-L (NF-L; cat. no. 2835; Cell Signaling Technology, Inc.) and reverse transcription-quantitative PCR (RT-qPCR). Western blotting for the expression of the RGC-specific markers, including Brn3a (cat. no. MAB1585 clone 5A3.2; EMD Millipore), thymus cell antigen 1 (Thy-1; cat. no. MAB1406; EMD Millipore) and NF-L was conducted as described previously (22,23). The use of animals and the experimental protocols performed were approved by the Animal Care Committee of The First Affiliated Hospital of Xinxiang Medical University (approval no. 2017-0163) in accordance with institutional guidelines. TMP hydrochloride (100 μM) was purchased from Harbin Medisan Pharmaceutical Co., dissolved in normal saline and diluted immediately prior to each experiment.

Establishment of a model of oxidative stress injury in PRGCs and TMP treatment. The PRGCs were cultured in DMEM supplemented with 10% fetal bovine serum (HyClone; GE Healthcare Life Sciences), 100 U/ml penicillin and streptomycin at 37˚C in a humidified atmosphere with 5% CO_2. The PRGCs were treated with different concentrations H_2O_2 (0, 100 200, 400 and 800 μM) at 37˚C for 16 h. Cell viability was tested to investigate cell injury induced by H_2O_2 in PRGCs, and 400 μM H_2O_2 was selected to establish the model of oxidative stress injury in PRGCs.

PRGCs were pre-treated with TMP at different dosages (25, 50 and 100 μM) at 37˚C for 24 h. The cells were then subjected to oxidative insult with H_2O_2 (400 μM) at 37˚C for 16 h and collected for subsequent experiments. Blank cells comprised untreated cells and the control or vehicle was that of cells treated with H_2O_2 or H_2O_2 + DMSO (1% v/v), respectively.

Cell viability. PRGCs ($1x10^4$ cells) were seeded into 96-well plates and cultured overnight at 37˚C in a humidified tissue culture incubator with 5% CO_2. At the end of treatment, cell viability was determined using Cell Counting Kit-8 (CCK-8) assay (Dojindo Molecular Technologies, Inc.). Briefly, 10 μl CCK-8 reagent (Dojindo Molecular Technologies, Inc.) was added to each well, then the cells were incubated for 3 h at 37˚C. The absorbance of the samples was read at 450 nm with a microplate reader (Sunrise™; Tecan Group, Ltd.).

Caspase-3 activity assay. At the end of TMP treatment, the activity of caspase-3 was measured with a caspase-3 assay kit (Abcam) according to the manufacturer's protocols. The samples were analyzed using a microplate reader (Model 680, Bio-Rad Laboratories, Inc.) at 405 nm.

Detection of apoptosis by flow cytometry. PRGCs were seeded in 6-well plates at a density of $1.0x10^6$ cell/well. Following treatment with TMP, the cells were washed twice with PBS, and then fixed in 70% ice-cold ethanol in PBS at 4˚C for 30 min. Subsequently, the cells were stained with 5 μl Annexin V-fluorescein isothiocyanate and 1 μl of propidium iodide (Bio-Science, Co. Ltd.). After incubation for 15 min at room temperature in the dark, cell apoptosis was analyzed with a FACScan flow cytometer (FCM; Beckman Coulter, Inc.). FlowJo software version 7.6.1 (FlowJo LLC, USA) was used to analyze flow cytometry data.

Reactive oxygen species (ROS) detection. ROS production in PRGCs was analyzed using 2',7'-dichlorofluorescin-diacetate (DCHF-DA; cat. no. D6883, Sigma-Aldrich; Merck KGaA). Briefly, PRGCs were incubated with 10 μM DCHF-DA for 30 min at 37˚C, followed by two washes with PBS. Then, the DCFH-DA staining for the detection of ROS production was observed using a fluorescence microscope (Nikon Corporation). Fluorescence was read at 485 nm for excitation and 530 nm for emission with an Infinite M200 Microplate Reader (Tecan Group, Ltd.).

ELISA. The concentrations of malondialdehyde (MDA) and superoxide dismutase (SOD) in the conditioned media were analyzed by an MDA Assay kit (cat. no. MAK085) and SOD Assay kit (cat. no. 19160) from Sigma-Aldrich (Merck KGaA) according to the manufacturer's protocols.

RT-qPCR. Following treatment, total RNA was extracted from retinal tissues or cultured cells using a miRNAeasy mini kit (Qiagen, Inc.) according to the manufacturer's protocols. A total of 200 ng of RNA was reverse-transcribed with a miRNA reverse transcription kit (Qiagen, Inc.) and an mRNA RT kit (Invitrogen; Thermo Fisher Scientific, Inc.), respectively. qPCR was performed using the iTaqTM Universal SYBR Green Supermix (Bio-Rad Laboratories, Inc.) on a 7500HT Real-Time PCR System (Thermo Fisher Scientific, Inc.). Relative expression levels were quantified via normalization to small nuclear (sno)RNA202. The primers employed for

qPCR were as follows: miR-182 5'-TGCGCTTTGGCAATG GTAGAACTC-3' (forward) 5'-CCAGTGCAGGGTCCG AGGTATT-3' (reverse); miR-34a 5'-ACACTCCAGCTGGGT GGCAGTGTCTTAGCT-3' (forward), 5'-CTCAACTGG TGTCGTGGA-3' (reverse); miR-150 5'-TCTCCCAACCCT TGTACCAGTG-3' (forward) 5'-CTCAACTGGTGTCGTG GTA-3' (reverse); miR-214 5'-ATAGAATTCTTTCTCCCTTT CCCCTTACTCTCC-3' (forward) 5'-CCAGGATCCTTTCAT AGGCACCACTCACTTTAC-3' (reverse); miR-137 5'-GCA GCAAGAGTTCTGGTGGC-3' (forward), 5'-TGGAACCAG TGCGAAAACAC-3' (reverse); miR-210 5'-GTGCAGGGT CCGAGGT-3' (forward), 5'-CTGTGCGTGTGACAGCGGCT GA-3' (reverse); snoRNA202 5'-GTCGTATCCAGTGCAGGG TCCGAGGTATTCGCACTGGATACGACCATCAG-3' (RT), 5'-GCAGGGTCCGAGGTATTC-3' (forward) and 5'-CTT GATGAAAGTACTTTTGA-3' (reverse). Brn3a 5'-TGGCGT CCATCTGCGATC-3' (forward); 5'-CTCAGGTTGTTC ATTTTTC-3' (reverse). Thy-1 5'-CGCTTTATCAAGGTC CTTACTC-3' (forward) 5'-GCGTTTTGAGATATTTGAA GGT-3' (reverse). NF-L 5'-ATGCTCAGATCTCCGTGGAG ATG-3' (forward); 5'-GCTTCGCAGCTCATTCTCCAGTT-3' (reverse). and GAPDH 5'-CATCAAGAAGGTGGTGAA GCAGG-3' (forward); 5'-CCACCACCCTGTTGCTGTAG CCA-3' (reverse). The reaction conditions were as follows: 94˚C for 5 min, followed by 40 cycles of 94˚C for 1 min, 56˚C for 1 min and 72˚C for 1 min. RT-qPCR assays were performed in triplicate and the changes in expression levels were calculated using the $2^{-\Delta\Delta Cq}$ method (24).

Transfection. PRGCs ($5x10^3$) were seeded into each well of a 6-well plate for 24 h, and the cells were subsequently transfected with miR-182 mimics, miR-182 inhibitor or the corresponding control vectors synthesized by Shanghai GenePharma Co., Ltd., at a final concentration of 50 nM using Lipofectamine® 2000 (Invitrogen; Thermo Fisher Scientific, Inc.) following the manufacturer's instructions. The sequences are as follows: miR-182 mimics, 5'-UUUGGCAAUGGUAGA ACUCACACU-3'; mimics negative control (NC), 5'-UUCUCC GAACGUGUCACGUTT-3'; miR-182 inhibitor, 5'-AGUGUG AGUUCUACCAUUGCCAAA-3' and inhibitor NC, 5'-CAG UACUUUUGUGUAGUACAA-3'. After 24 h post-transfection, the cells were pre-treated with 100 μM TMP for 24 h, then subjected to oxidative insult with H_2O_2 (400 μM) at 37˚C for 16 h and collected for subsequent experiments.

Bioinformatics. TargetScan (version 7.0; www.targetscan.org/) and PicTar (release 2006; https://pictar.mdc-berlin.de) target gene prediction software were used to select MIF as a target gene of miR-182.

Luciferase reporter assay. The Bcl-2 interacting protein 3 (BNIP3) 3'-untranslated region (UTR) containing complementary sequences or the mutated sequence for the seed sequence of miR-182 was amplified by PCR as described previously (25), and cloned into the firefly luciferase expressing vector, pGL3 (Promega Corporation); the vectors were denoted as wild-type (wt) pGL3-BNIP3-3'-UTR and mutant (mut) BNIP3-3'-UTR, respectively. For the luciferase reporter assay, 293T cells (American Type Culture Collection) were seeded into a 24-well plate ($5.0x10^5$/well) and transfected with the wt or mut reporter vector, together with miR-182 mimics or miR-182 inhibitor using Lipofectamine 2000. At 48 h after transfection, the luciferase activity was determined by using a dual-luciferase reporter assay system (Promega Corporation). The pRL-TK plasmid (Promega Corporation) was used as a normalizing control. All experiments were performed in triplicate.

Western blotting. Total protein was extracted from PRGCs or retinal tissues using radioimmunoprecipitation assay lysis (Sigma-Aldrich; Merck KGaA) after treatments. The protein concentration was determined using a BCA protein assay kit (Pierce; Thermo Fisher Scientific, Inc.). Total protein samples (30 μg) were analyzed by 8% SDS-PAGE and transferred to a polyvinylidene fluoride membrane (EMD Millipore). β-actin was used for the normalization of protein expression. The membranes were blocked with 5% non-fat milk at 4˚C overnight, and incubated with primary antibodies overnight at 4˚C. Primary antibodies against Bcl-2-assoiated X protein (Bax; cat. no. sc-4239, 1:1,000), Bcl-2 (cat. no. sc-176463, 1:1,000), BNIP3 (cat. no. sc-1715, 1:1,000) and β-actin (cat. no. sc-8432, 1:2,000) were purchased from Santa Cruz Biotechnology, Inc., while cleaved (cle)-caspase-3 (cat. no. 9661, 1:1,000), cle-poly(ADP-ribose)polymerase (PARP; cat. no. 5625, 1:1,000), Cytochrome *c* (cyto c cat. no. 4280, 1:1,000) and Complex IV (cat. no. 4850, 1:1,000) were purchased from Cell Signaling Technology, Inc. After washing with PBS, the membrane was incubated with horseradish peroxidase-conjugated antibody (cat. no. ab205718; 1:2,000, Abcam) for 1 h at room temperature, and the bands were detected with an ECL Advance reagent (GE Healthcare). The intensity of the bands of interest was analyzed with ImageJ software version 1.46 (National Institutes of Health).

Mitochondrial membrane potential assay. After treatments, a commercial Mitochondrial Membrane Potential Assay kit with JC-1 (Invitrogen; Thermo Fisher Scientific, Inc.) was used to determine the mitochondrial membrane potential ($\Delta\Psi m$) according to the manufacturer's instructions. Briefly, after washing twice with PBS, PRGCs were stained with JC-1 (5 μg/ml) for 15 min at 37˚C. The red and green fluorescence intensities were detected (excitation wavelength of 488 nm and emission wavelength at 500 nm) using a Bio-Tek fluorescent microplate reader (BioTek Instruments, Inc.). The $\Delta\Psi m$ of the PRGCs in each treatment group was calculated as the ratio of red to green fluorescence and expressed as a multiple of the level in the control group.

Statistical analyses. SPSS 13.0 software (SPSS, Inc.) was used to analyze the data. Data were expressed as the mean ± standard deviation of three independent experiments. A Student's t-test was used to analyze differences between two groups. Differences between multiple groups were analyzed by one-way analysis of variance, followed by a Tukey's post-hoc test for multiple comparisons. $P<0.05$ was determined to indicate a statistically significant difference.

Results

TMP promotes cell viability and suppresses cell apoptosis in H_2O_2-treated PRGCs. At days 3 and 7 of the first passage, PRGCs were collected for immunofluorescence analysis of an

RGC marker. Membranous staining of NF-L was observed in the soma and neurites (Fig. 1A). To verify the purity of the isolated PRGC population, the expression levels of NF-L, Thy-1 and Brn3a (RGC markers) were detected by RT-qPCR. As presented in Fig. 1B-D, the expression levels of these markers were significantly increased in the isolated PRGCs compared with in retinal tissue. Similar results were observed via western blotting (Fig. 1E). These data demonstrated that the isolated neoplastic stromal cell populations were not contaminated by histiocytes or giant cells.

H_2O_2 is widely used to establish an oxidative injury model using RGCs to mimic the development of glaucoma *in vitro* (26,27). As presented in Fig. 1F, H_2O_2 significantly suppressed the viability of PRGCs in a dose-dependent manner; however, no significant difference in viability between 400 and 800 μM was observed. Based on previous reports (17,28,29), we used 400 μM H_2O_2 to generate a cell model of oxidative injury. To determine whether TMP promotes the growth of PRGCs, we treated cells with 25, 50 and 100 μM TMP for 24 h, followed by 400 μM H_2O_2. Subsequently, cell viability was evaluated by a CCK-8 assay. The results showed that TMP alleviated H_2O_2-induced suppression of cell viability, and this effect was does-dependent (Fig. 1G). Further investigation revealed that H_2O_2 significantly increased the activity of caspase-3 compared with in the control group, whereas TMP attenuated the promoting effects of H_2O_2 on caspase-3 activity (Fig. 1H). Consistent with these results, TMP also significantly attenuated H_2O_2-induced cell apoptosis (Fig. 1I). Of note, 100 μM TMP was used for subsequent experiments and this concentration has also been used previously (17,28,29). Collectively, these results indicated that the oxidative injury model of PRGCs was successfully established and TMP treatment could improve H_2O_2-induced cell damage.

TMP attenuates H_2O_2-induced oxidative damage in PRGCs. It has been acknowledged that glaucoma is associated with oxidative stress, which can lead to the apoptosis of RGCs (4,5). MDA is a biomarker of oxidative stress of cells; SOD is the main antioxidative enzyme and can resist the damage of oxygen-free radicals to cells (30). Therefore, in the present study, the levels of ROS, MDA and SOD were examined to assess the protective effects of TMP in H_2O_2-treated PRGCs. As presented in Fig. 2A and B, H_2O_2 treatment significantly increased intracellular ROS levels compared with in Blank cells. However, pretreatment with TMP significantly decreased ROS levels in a dose-dependent manner. It was also observed that H_2O_2 treatment significantly increased the levels of MDA and decreased the levels of SOD compared with that in Blank cells, but these effects were significantly attenuated by TMP (Fig. 2C and D). Our findings suggested that TMP attenuated H_2O_2-induced cell damage by reducing oxidative stress.

TMP upregulated the expression of miR-182. Recently, ROS has been reported to alter the expression of certain miRNAs (31,32). Given TMP suppressed the accumulation of ROS, we hypothesized that TMP exerts its protective effects against H_2O_2-induced cell injury via the regulation of miRNAs. Thus, we investigated the regulatory effects of TMP on the changes in the expression of miRNAs, which have been reported be altered in response to ROS exposure previously (33). The results of RT-qPCR showed that H_2O_2 significantly increased the expression of miR-214 and miR-210, and decreased the expression of miR-182 and miR-137, compared with control group, which corresponds with previous studies (34-37). Interestingly, the expression levels of miR-150 and miR-34a were markedly unaltered after H_2O_2 treatment, which differs with previous reports (38,39); this may be due to the use of different cell lines. Of note, the expression of miR-182 in H_2O_2-treated PRGCs was significantly downregulated compared with the control, but increased in response to TMP; however, no significant changes were observed in the expression of miR-214, miR-137 and miR-210 following TMP treatment (Fig. 3A-F). These findings prompted us to investigate the role of miR-182 in TMP-mediated protective effects against H_2O_2-induced cell damage.

Knockdown of miR-182 inhibits the protective effects of TMP in H_2O_2-induced cell damage. Previous studies have been reported that miR-182 possesses potent antioxidative and antiapoptotic activity in a variety of diseases (33,35). To investigate whether ectopic expression of miR-182 involves the protective effects of TMP on H_2O_2-induced cell damage, miR-182 inhibitor or miR-182 mimics were transfected into PRGCs prior to H_2O_2 and TMP treatment. As presented in Fig. 4A, miR-182 expression was significantly decreased and increased after miR-182 inhibitor or miR-182 mimics transfection in PRGCs, respectively. It was observed that miR-182 knockdown significantly alleviated the protective effects of TMP in H_2O_2-treated PRGCs, by reducing cell viability and inducting apoptosis (Fig. 4B and C). The intracellular ROS levels in the H_2O_2 + TMP + miR-182 inhibitor group were significantly higher than H_2O_2 + TMP group (Fig. 4D). In addition, as shown in Fig. 4E and F, the levels of MDA were significantly increased and the levels of SOD were decreased in the H_2O_2 + TMP + miR-182 inhibitor group, compared with that of the H_2O_2 + TMP group. These findings suggested that miR-182 knockdown suppressed the protective effects of TMP in H_2O_2-induced injury.

BINP3 is a direct target of miR-182. To explore the molecular mechanism by which miR-182 functions in the protective effects of TMP in H_2O_2-induced injury, we performed TargetsScan and PicTar analyses to predict the target genes of miR-182 and identified BNIP3 as a potential target of miR-182, with the target site located in the 3'-UTR (Fig. 5A). To validate this bioinformatic predication, we established the luciferase reporter plasmids containing the wt or mut 3'-UTR segments of BNIP3. The luciferase reporter assay revealed that miR-182 mimics significantly inhibited the luciferase activity compared with the mimic NC, while miR-182 inhibitor significantly enhanced the luciferase activity compared with the inhibitor NC (Fig. 5B). Additionally, miR-182 mimics or inhibitor did not markedly affect luciferase activity when the targeted BNIP3 sequence was mutated in the miR-182-binding site (Fig. 5B). To further confirm that BNIP3 expression is regulated by miR-182, BNIP3 protein expression was analyzed by western blotting. We found that the expression levels of BNIP3 were notably downregulated by miR-182 mimics, but markedly enhanced by miR-182 inhibitor (Fig. 5C). Taken together,

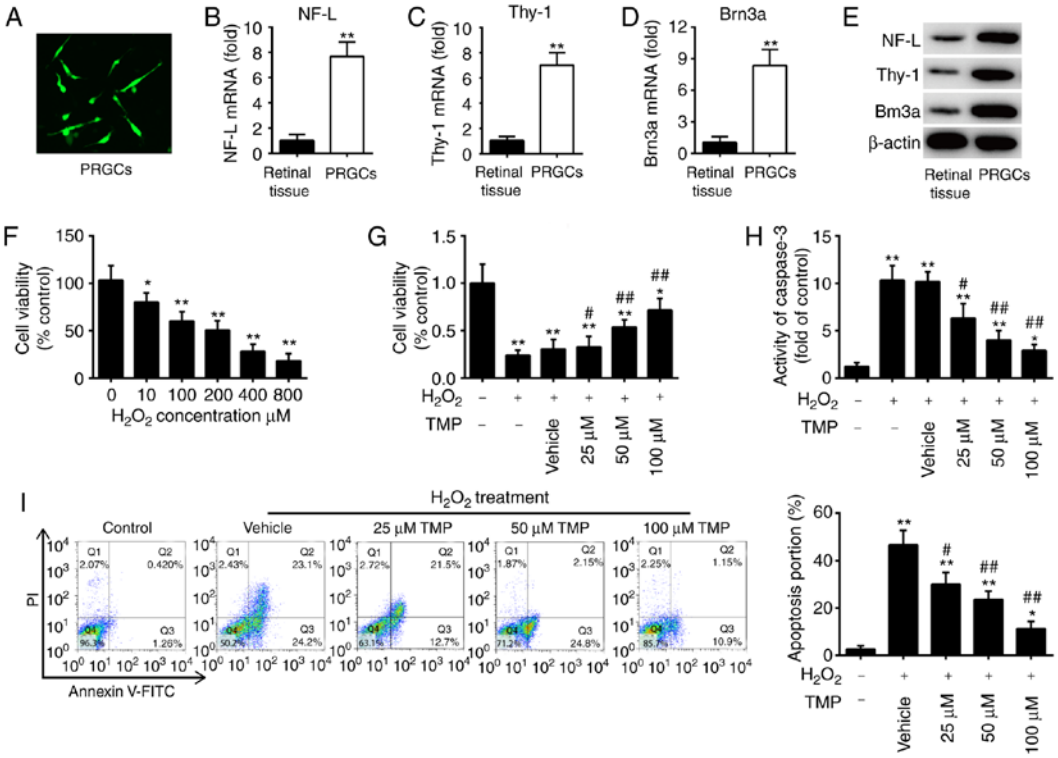

Figure 1. TMP promotes cell viability and suppresses cell apoptosis in H_2O_2-treated PRGCs. (A) NF-L expression was detected by immunofluorescence (magnification, x200). (B-D) The mRNA expression levels of NF-L, Thy-1 and Brn3a were measured by reverse transcription-quantitative PCR. (E) Protein expression of NF-L, Thy-1 and Brn3a as determined by western blotting. β-actin was used as a loading control. (F) PRGCs were treated with 10, 100, 200, 400 and 800 μM of H_2O_2 for 24 h, and then cell viability was determined by a CCK-8 assay. PRGCs were pre-treated with 25, 50 and 100 μM TMP for 24 h prior to exposure with 400 μM of H_2O_2. (G) Cell viability was determined by a CCK-8 assay. (H) The activity of caspase-3 was determined using a caspase-3 assay kit. (I) Apoptosis was detected via flow cytometric analysis. Data are presented as mean of three replicates ± standard deviation. *P<0.05, **P<0.01 vs. Control group, $^{\#}$P<0.05, $^{\#\#}$P<0.01 vs. Vehicle + H_2O_2 group. CCK-8, Cell Counting Kit-8; FITC, fluorescein isothiocyanate; NF-L, neurofilament-L; PI, propidium iodide; PRGCs, primary retinal ganglion cells; Thy-1, thymus cell antigen 1; TMP, tetramethylpyrazine.

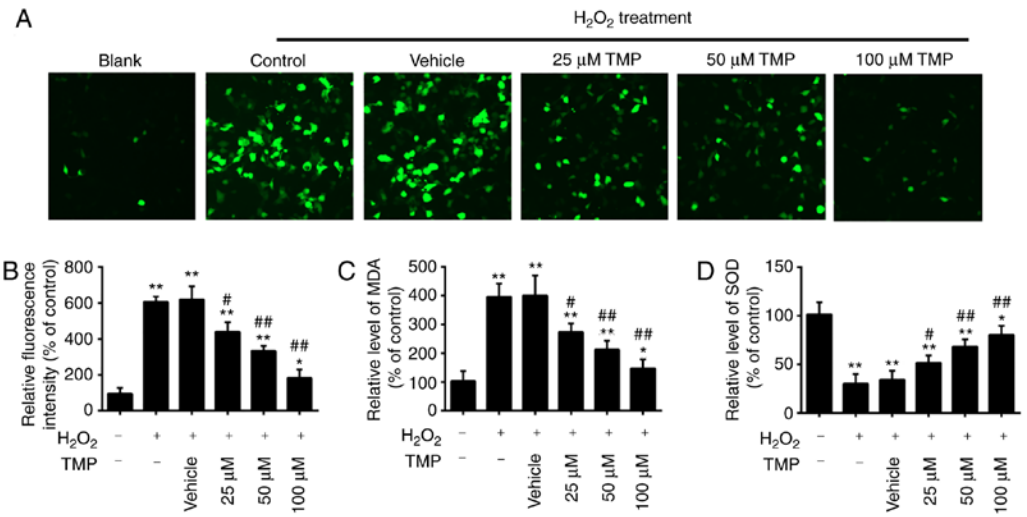

Figure 2. TMP attenuates H_2O_2-induced oxidative damage in PRGCs. PRGCs were pre-treated with 25, 50 and 100 μM of TMP for 24 h prior to being exposed to 400 μM of H_2O_2. (A and B) ROS production was measured by a 2',7'-dichlorofluorescin-diacetate assay (magnification, x200). (C and D) The levels of MDA and SOD were detected by an ELISA assay. Data are presented as the mean of three replicates ± standard deviation. *P<0.05, **P<0.01 vs. Control group, $^{\#}$P<0.05, $^{\#\#}$P<0.01 vs. Vehicle + H_2O_2 group. PRGCs, primary retinal ganglion cells; MDA, malondialdehyde; SOD, superoxide dismutase; TMP, tetramethylpyrazine.

these findings indicated that miR-182 inhibit the expression of BNIP3, further suggesting that the miR-182/BNIP3 axis may be involved in the protective effects of TMP in H_2O_2-induced injury.

TMP attenuates H_2O_2-induced PRGC apoptosis via the miR-182/mitochondrial apoptotic pathway. BNIP3 is a well-known effector of the mitochondria-mediated apoptosis, which induces the formation of the pathological mitochondrial

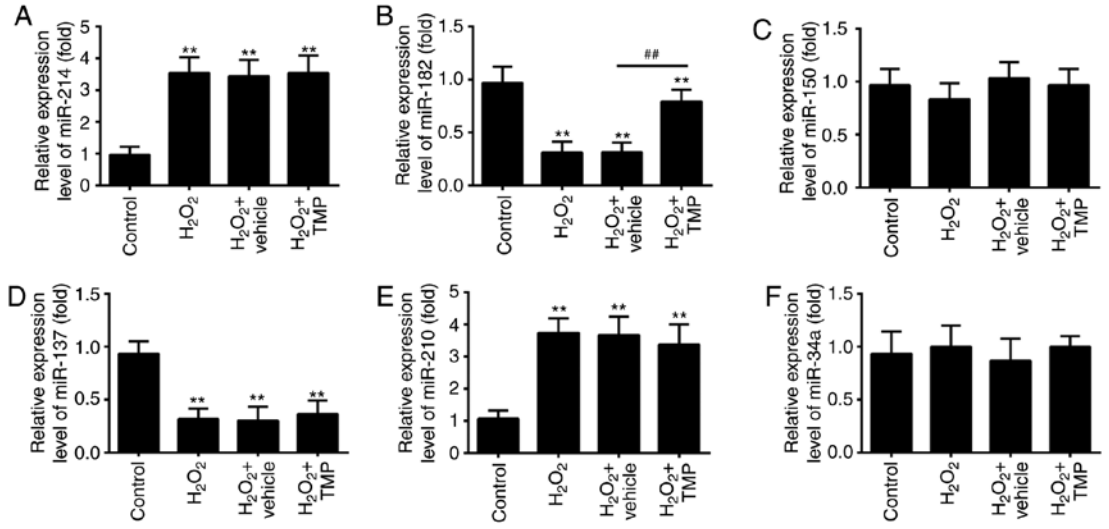

Figure 3. TMP upregulates the expression of miR-182. Primary retinal ganglion cells were pre-treated with TMP for 24 h prior to being exposed to 400 μM of H_2O_2. The expression levels of (A) miR-214, (B) miR-182, (C) miR-150, (D) miR-137, (E) miR-210 and (F) miR-34a were determined by reverse transcription-quantitative PCR. Data are presented as the mean of three replicates ± standard deviation. **P<0.01 vs. Control group, $^{\#\#}$P<0.01 vs. Vehicle + H_2O_2 group. miR, microRNA; TMP, tetramethylpyrazine.

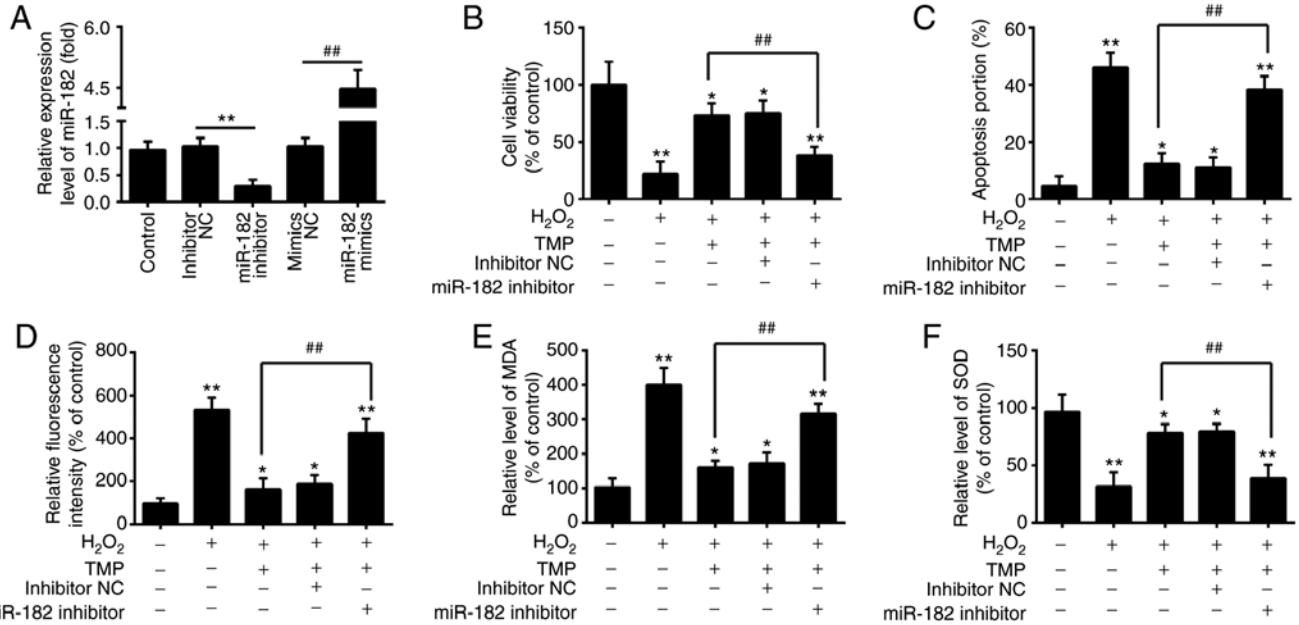

Figure 4. Knockdown of miR-182 inhibits the protective effects of TMP in H_2O_2-induced cell damage. (A) The expression of miR-182 was measured by reverse transcription-quantitative PCR after miR-182 inhibitor or miR-182 mimics transfection. Data are presented as the mean of three replicates ± standard deviation. **P<0.01 vs. inhibitor NC group, $^{\#\#}$P<0.01 vs. mimics NC group. Cells were transfected with miR-182 inhibitor or inhibitor NC before treatment with TMP for 24 h, and then exposed to H_2O_2. (B) Cell viability was then determined by a Cell Counting Kit-8 assay. (C) Apoptosis was detected by flow cytometric analysis. (D) ROS production was measured by a 2',7'-dichlorofluorescin-diacetate assay. (E and F) The levels of MDA and SOD were detected by an ELISA assay. Data are presented as the mean of three replicates ± standard deviation. *P<0.05, **P<0.01 vs. Control group, $^{\#\#}$P<0.01 vs. H_2O_2 + TMP group. MDA, malondialdehyde; miR, microRNA; NC, negative control; ROS, reactive oxygen species; SOD, superoxide dismutase; TMP, tetramethylpyrazine.

permeability transition pore (40,41). Thus, we sought to determine whether TMP could regulate the mitochondrial apoptotic pathway via the miR-182/BNIP3 axis. Western blotting was performed to detect the expression levels of apoptosis-related proteins in PRGCs transfected with miR-182 inhibitor prior to H_2O_2 and TMP treatment. As presented in Fig. 6A, H_2O_2 treatment significantly increased the expression of pro-apoptotic proteins (BNIP3, Bax, cle-caspase-3 and cle-PARP) and decreased that of anti-apoptotic Bcl-2, compared with the control group. Of note, the levels of these pro-apoptotic proteins were suppressed, whereas the anti-apoptotic protein was upregulated after TMP pretreatment. However, these effects of TMP were attenuated by miR-182 inhibitor. cyto c release from mitochondria into the cytosol is a critical event in apoptosis (42). Therefore, we further detected the effects of TMP on cyto c release. The data showed that H_2O_2 treatment induced the release of cyto c from the mitochondria, which was attenuated by TMP. However, the inhibitory

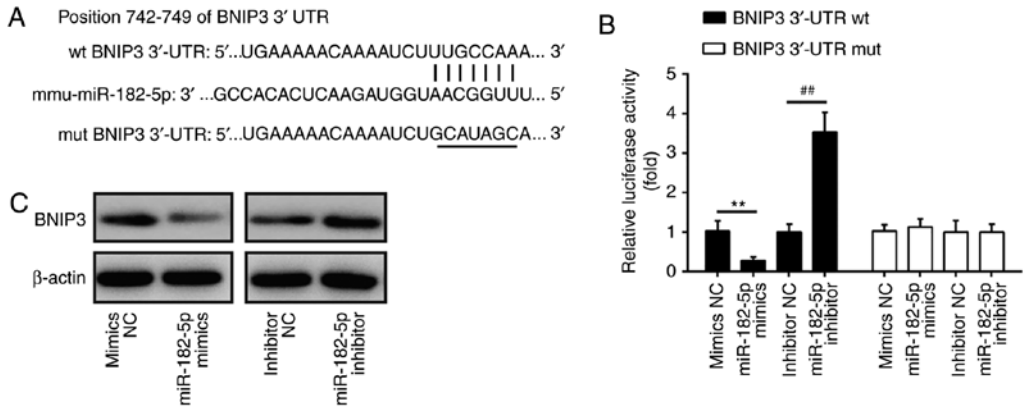

Figure 5. BNIP3 is a direct target of miR-182. (A) The putative binding site of miR-182 and BNIP3; (B) a luciferase assay of 293 co-transfected with firefly luciferase constructs containing the BNIP3 wt or mut 3'-UTR and miR-182 mimics, mimic NC, miR-182 inhibitor or inhibitor NC (n=3). Data are presented as the mean of three replicates ± standard deviation. **P<0.01 vs. mimics NC, $^{\#\#}$P<0.01 vs. inhibitor NC. (C) The expression of BNIP3 protein after transfection with miR-182 mimic or miR-182 inhibitor, as measured by western blotting. β-actin was used as a loading control. BNIP3, Bcl-2 interacting protein 3; miR, microRNA; mut, mutated; NC, negative control; UTR, untranslated region; wt, wild-type.

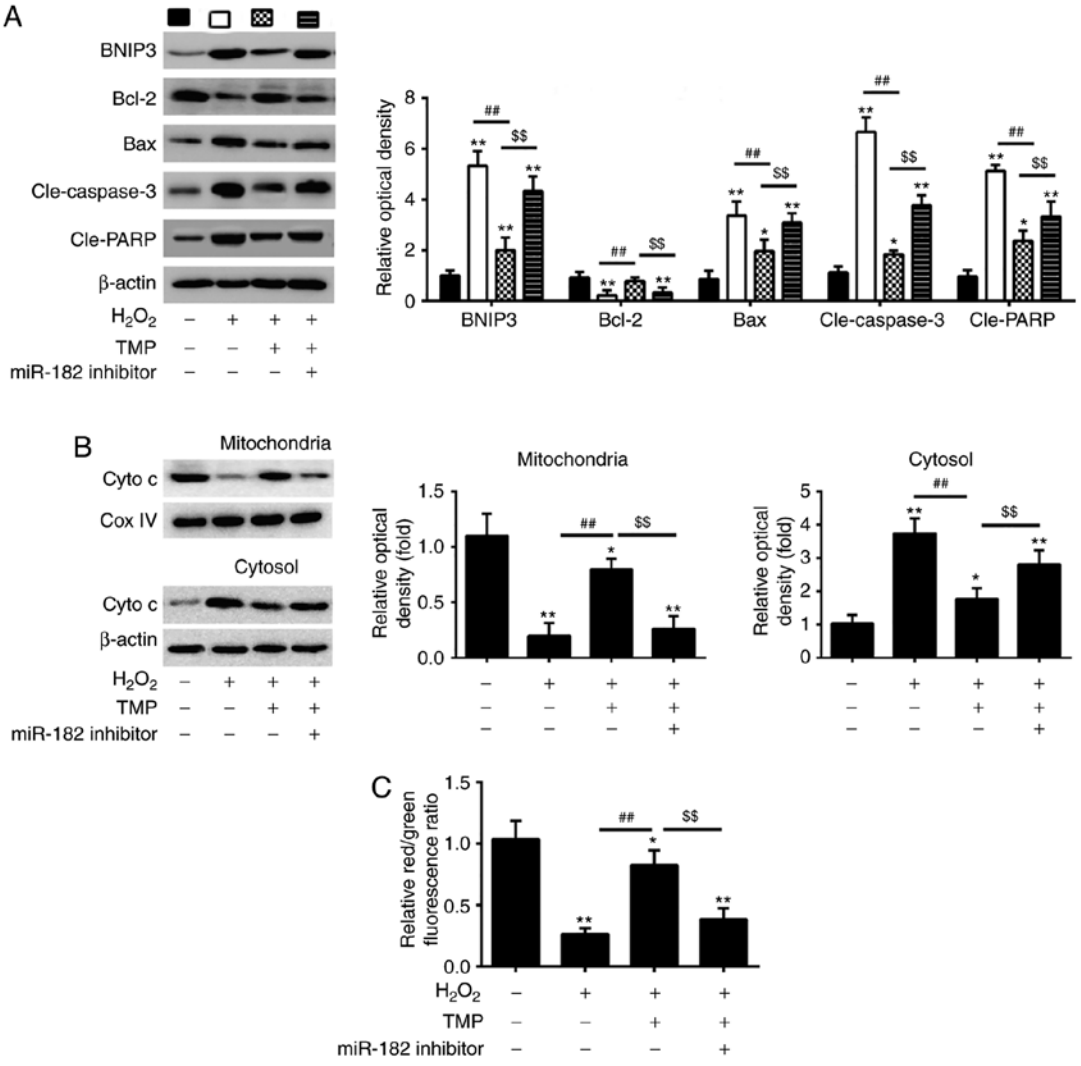

Figure 6. TMP attenuates H_2O_2-induced PRGC apoptosis via miR-182/mitochondrial apoptotic pathway. Cells were transfected with miR-182 inhibitor or inhibitor NC prior to treatment with TMP for 24 h and then exposed to H_2O_2. (A) Western blot analysis was conducted to determine the expression of apoptosis-related proteins (BNIP3, Bcl-2, cle-caspase-3, Bax and cle-PARP and Bcl-2). (B) Protein levels of cyto c in mitochondria and cytosol was measured using western blot analysis. β-actin and Cox IV were used as loading controls for the cytosolic and mitochondrial fractions, respectively. (C) Mitochondrial membrane potential levels in the treated PRGCs were analyzed using the JC-1 fluorescent probe. Data are presented as the mean of three replicates ± standard deviation. *P<0.05, **P<0.01 vs. Control group, $^{\#\#}$P<0.01 vs. H_2O_2 group, $^{\$\$}$P<0.01 vs. H_2O_2 + TMP group. Bcl-2, B-cell lymphoma 2; Bax, Bcl-2-assoiated X protein; BNIP3, Bcl-2 interacting protein 3; cle, cleaved; Cox, IV, Complex IV; Cyto c, cytochrome *c*; miR, microRNA; PARP, poly(ADP-ribose)polymerase; PRGCs, primary retinal ganglion cells; TMP, tetramethylpyrazine.

effects of TMP were significantly reversed by knockdown of miR-182 (Fig. 6B). In addition, whether TMP could reduce the H_2O_2-induced Δψm loss was investigated as dysregulated mitochondrial function causes the loss of Δψm. As presented in Fig. 6C, H_2O_2 treatment resulted in decreased red/green fluorescence ratio, which indicated that Δψm had dissipated, whereas TMP pretreatment attenuated H_2O_2-induced Δψm loss. However, knockdown of miR-182 significantly suppressed the promoting effects of TMP on Δψm. These results suggest that TMP may attenuate H_2O_2-induced PRGC apoptosis via the miR-182/mitochondrial apoptotic pathway.

Discussion

To the best of our knowledge, the present study is the first to demonstrate that TMP could attenuate H_2O_2-induced damage in PRGCs by suppressing apoptosis and oxidative stress. Additionally, we reported that TMP increased the expression of miR-182 and that miR-182 mediated the protective functions of TMP in H_2O_2-induced damage by targeting BNIP3 via inhibiting the mitochondrial apoptotic pathway. Therefore, our findings suggest that TMP may be a potential therapeutic agent for the treatment of glaucoma.

Previously, TMP has been reported to exhibit neuroprotective effects against retinal diseases in a number of *in vitro* and *in vivo* studies (43-45). Wang *et al* (46) found that the protective effects of TMP against all-trans-retinal toxicity in differentiated Y-79 cells, an *in vitro* model of photoreceptors, were mediated via upregulation of interphotoreceptor retinoid-binding protein expression. Yu *et al* (47) revealed that TMP attenuated transforming growth factor-β-induced pathological changes in the trabecular meshwork through the C-X-C chemokine receptor type 4 pathway, indicating that TMP is a potential therapeutic method for treating primary open-angle glaucoma; the roles of TMP in glaucoma require further investigation. The present study extensively evaluated the protective effects of TMP against H_2O_2-induced damage in PRGCs, an *in vitro* model of glaucoma. The results showed that TMP pre-treatment attenuated H_2O_2 induced PRGC injury, as suggested by increases in cell viability, reductions in the activity of caspase-3 and cell apoptosis, as well as the low levels of ROS, the high levels of MDA and the low level of SOD. Collectively, these results indicated that TMP treatment exerts its protective effects against H_2O_2-induced damage through suppressing apoptosis and oxidative stress.

It has been proposed that oxidative stress is an important mechanism involved in triggering RGC apoptosis in glaucoma (48); however, the precise nature of RGC damage caused by oxidative stress remains unclear. Emerging evidence suggests that ROS can modulate the expression of some miRNAs in many diseases (49,50). For example, miR-181a has been shown to be upregulated upon treatment with 600 μM H_2O_2 in rat bone marrow mesenchymal stem cells and this increased expression induced cell death (51). In this study, TMP could inhibit ROS production; thus, the protective effects of TMP in H_2O_2-induced injury may be mediated by miRNAs induced by ROS. In the present study, a total of six differentially expressed miRNAs that were associated with ROS were screened out, in which the levels of miR-182 were significantly downregulated upon exposure to H_2O_2, but were upregulated following treatment with TMP.

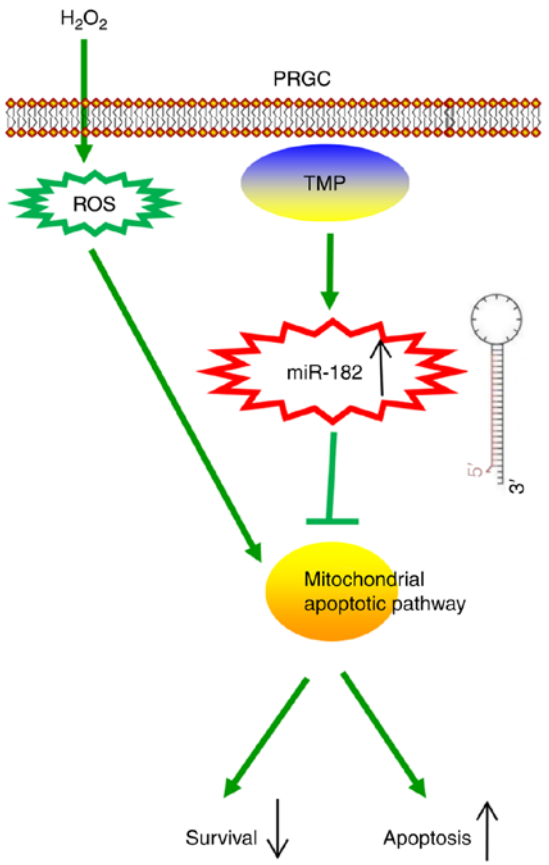

Figure 7. Schematic diagram of the signaling pathway in which TMP suppresses H_2O_2-induced damage in PRGCs. TMP ameliorated H_2O_2-induced damage in PRGCs via the miR-182/mitochondria apoptotic pathway. miR, microRNA; PRGC, primary retinal ganglion cell; ROS, reactive oxygen species; TMP, tetramethylpyrazine.

Interestingly, the literature shows miR-182 to be involved in anti-apoptotic and antioxidative processes (52,53). For example, miR-182 inhibited oxidative stress and apoptosis induced by oxidized low-density lipoprotein via targeting Toll-like receptor 4 in RAW264.7 cells (35). Thus, we investigated whether TMP attenuated H_2O_2-induced damage via regulating miR-182. As expected, suppression of miR-182 abolished the protective effects of TMP on H_2O_2-induced damage; however, how miR-182 functions in the protective effects of TMP remains unknown.

We explored the underlying molecular mechanism responsible for the protective effects of TMP in H_2O_2-induced damage. Based on bioinformatics analysis and the dual-luciferase reporter assay, our results showed that miR-182 could directly target BNIP3, an effector of mitochondria-mediated apoptosis (54-56). Therefore, the protective effects of TMP on H_2O_2-induced damage may be mediated by the miR-182/mitochondria apoptotic pathway. In this study, our results demonstrated that TMP downregulated BNIP3, cleaved-caspase-3, Bax and cleaved-PARP, and increased Bcl-2 expression in the H_2O_2-treated PRGCs. However, these effects were attenuated by miR-182 inhibition. Furthermore, TMP attenuated H_2O_2-induced release of cyto c and alleviated dissipated Δψm. Similarly, these effects were attenuated by miR-182 inhibition. Taken together, these findings indicated that TMP exerts its protective effects on H_2O_2-induced damage via modulating the miR-182/mitochondria apoptotic pathway.

In conclusion, the present study revealed that TMP improved H_2O_2-induced damage in PRGCs via the miR-182/mitochondria apoptotic pathway (Fig. 7). Our findings suggest that TMP may be considered as a candidate therapeutic agent for the prevention and treatment of glaucoma. However, the application and efficacy of TMP in clinical practice requires further investigation.

Acknowledgements

Not applicable.

Funding

No funding was received.

Availability of data and materials

All data generated or analyzed during this study are included in this published article.

Authors' contributions

XL, QW, YR, XW, HC, HY and BW performed the experiments, contributed to data analysis and wrote the paper. HY and BW made substantial contributions to the design of the present study, contributed to data analysis and acquired experimental materials. All authors read and approved the final manuscript.

Ethics approval and consent to participate

The use of animals and the experimental protocols performed were approved by the Animal Care Committee of The First Affiliated Hospital of Xinxiang Medical University (approval no. 2017-0163) in accordance with institutional guidelines.

Patient consent for publication

Not applicable.

Competing interests

The authors declare that they have no competing interests.

References

1. Koriyama Y, Ohno M, Kimura T and Kato S: Neuroprotective effects of 5-S-GAD against oxidative stress-induced apoptosis in RGC-5 cells. Brain Res 1296: 187-195, 2009.
2. Tham YC, Li X, Wong TY, Quigley HA, Aung T and Cheng CY: Global prevalence of glaucoma and projections of glaucoma burden through 2040: A systematic review and meta-analysis. Ophthalmology 121: 2081-2090, 2014.
3. Lee D, Shim MS, Kim KY, Noh YH, Kim H, Kim SY, Weinreb RN and Ju WK: Coenzyme Q10 inhibits glutamate excitotoxicity and oxidative stress-mediated mitochondrial alteration in a mouse model of glaucoma. Invest Ophthalmol Vis Sci 55: 993-1005, 2014.
4. Sancho P, Fernández C, Yuste VJ, Amrán D, Ramos AM, de Blas E, Susin SA and Aller P: Regulation of apoptosis/necrosis execution in cadmium-treated human promonocytic cells under different forms of oxidative stress. Apoptosis 11: 673-686, 2006.
5. Almasieh M, Wilson AM, Morquette B, Cueva Vargas JL and Di Polo A: The molecular basis of retinal ganglion cell death in glaucoma. Prog Retin Eye Res 31: 152-181, 2012.
6. Zhai L, Zhang P, Sun RY, Liu XY, Liu WG and Guo XL: Cytoprotective effects of CSTMP, a novel stilbene derivative, against H2O2-induced oxidative stress in human endothelial cells. Pharmacol Rep 63: 1469-1480, 2011.
7. Wu J, Song R, Song W, Li Y, Zhang Q, Chen Y, Fu Y, Fang W, Wang J, Zhong Z, *et al*: Chlorpromazine protects against apoptosis induced by exogenous stimuli in the developing rat brain. PLoS One 6: e21966, 2011.
8. Tang Z, Wang Q, Xu H and Zhang W: Microdialysis sampling for investigations of tetramethylpyrazine following transdermal and intraperitoneal administration. Eur J Pharm Sci 50: 454-458, 2013.
9. Gong X, Wang Q, Tang X, Wang Y, Fu D, Lu H, Wang G and Norgren S: Tetramethylpyrazine prevents contrast-induced nephropathy by inhibiting p38 MAPK and FoxO1 signaling pathways. Am J Nephrol 37: 199-207, 2013.
10. Yang G, Qian C, Wang N, Lin C, Wang Y, Wang G and Piao X: Tetramethylpyrazine protects against oxygen-glucose deprivation-induced brain microvascular endothelial cells injury via Rho/Rho-kinase signaling pathway. Cell Mol Neurobiol 37: 619-633, 2017.
11. Lu C, Zhang J, Shi X, Miao S, Bi L, Zhang S, Yang Q, Zhou X, Zhang M, Xie Y, *et al*: Neuroprotective effects of tetramethylpyrazine against dopaminergic neuron injury in a rat model of Parkinson's disease induced by MPTP. Int J Biol Sci 10: 350-357, 2014.
12. Zhong M, Ma W, Zhang X, Wang Y and Gao X: Tetramethyl pyrazine protects hippocampal neurons against anoxia/reoxygenation injury through inhibiting apoptosis mediated by JNK/MARK signal pathway. Med Sci Monit 22: 5082-5090, 2016.
13. Luo X, Yu Y, Xiang Z, Wu H, Ramakrishna S, Wang Y, So KF, Zhang Z and Xu Y: Tetramethylpyrazine nitrone protects retinal ganglion cells against N-methyl-d-aspartate-induced excitotoxicity. J Neurochem 141: 373-386, 2017.
14. Ambros V: The functions of animal microRNAs. Nature 431: 350-355, 2004.
15. Bartel DP: MicroRNAs: Genomics, biogenesis, mechanism, and function. Cell 116: 281-297, 2004.
16. Guo R, Shen W, Su C, Jiang S and Wang J: Relationship between the Pathogenesis of Glaucoma and miRNA. Ophthalmic Res 57: 194-199, 2017.
17. Kong N, Lu X and Li B: Downregulation of microRNA-100 protects apoptosis and promotes neuronal growth in retinal ganglion cells. BMC Mol Biol 15: 25, 2014.
18. Li H, Zhu Z, Liu J, Wang J and Qu C: MicroRNA-137 regulates hypoxia-induced retinal ganglion cell apoptosis through Notch1. Int J Mol Med 41: 1774-1782, 2018.
19. Zhang QL, Wang W, Alatantuya, Dongmei, Lu ZJ, Li LL and Zhang TZ: Down-regulated miR-187 promotes oxidative stress-induced retinal cell apoptosis through P2X7 receptor. Int J Biol Macromol 120: 801-810, 2018.
20. Cheng LB, Li KR, Yi N, Li XM, Wang F, Xue B, Pan YS, Yao J, Jiang Q and Wu ZF: miRNA-141 attenuates UV-induced oxidative stress via activating Keap1-Nrf2 signaling in human retinal pigment epithelium cells and retinal ganglion cells. Oncotarget 8: 13186-13194, 2017.
21. Jiao J, Huang X, Feit-Leithman RA, Neve RL, Snider W, Dartt DA and Chen DF: Bcl-2 enhances Ca(2+) signaling to support the intrinsic regenerative capacity of CNS axons. EMBO J 24: 1068-1078, 2005.
22. Rodriguez AR, de Sevilla Müller LP and Brecha NC: The RNA binding protein RBPMS is a selective marker of ganglion cells in the mammalian retina. J Comp Neurol 522: 1411-1443, 2014.
23. Zhang XM, Li Liu DT, Chiang SW, Choy KW, Pang CP, Lam DS and Yam GH: Immunopanning purification and long-term culture of human retinal ganglion cells. Mol Vis 16: 2867-2872, 2010.
24. Livak KJ and Schmittgen TD: Analysis of relative gene expression data using real-time quantitative PCR and the 2(-Delta Delta C(T)) method. Methods 25: 402-408, 2001.
25. Lee SY, Lee S, Choi E, Ham O, Lee CY, Lee J, Seo HH, Cha MJ, Mun B, Lee Y, *et al*: Small molecule-mediated up-regulation of microRNA targeting a key cell death modulator BNIP3 improves cardiac function following ischemic injury. Sci Rep 6: 23472, 2016.

26. Ju WK, Liu Q, Kim KY, Crowston JG, Lindsey JD, Agarwal N, Ellisman MH, Perkins GA and Weinreb RN: Elevated hydrostatic pressure triggers mitochondrial fission and decreases cellular ATP in differentiated RGC-5 cells. Invest Ophthalmol Vis Sci 48: 2145-2151, 2007.
27. Liu Q, Ju WK, Crowston JG, Xie F, Perry G, Smith MA, Lindsey JD and Weinreb RN: Oxidative stress is an early event in hydrostatic pressure induced retinal ganglion cell damage. Invest Ophthalmol Vis Sci 48: 4580-4589, 2007.
28. Lv B, Chen T, Xu Z, Huo F, Wei Y and Yang X: Crocin protects retinal ganglion cells against H2O2-induced damage through the mitochondrial pathway and activation of NF-κB. Int J Mol Med 37: 225-232, 2016.
29. Zhang QL, Wang W, Jiang Y, A-Tuya, Dongmei, Li LL, Lu ZJ, Chang H and Zhang TZ: GRGM-13 comprising 13 plant and animal products, inhibited oxidative stress induced apoptosis in retinal ganglion cells by inhibiting P2RX7/p38 MAPK signaling pathway. Biomed Pharmacother 101: 494-500, 2018.
30. Chen H, Chow PH, Cheng SK, Cheung AL, Cheng LY and O WS: Male genital tract antioxidant enzymes: Their source, function in the female, and ability to preserve sperm DNA integrity in the golden hamster. J Androl 24: 704-711, 2003.
31. Lin J, Chuang CC and Zuo L: Potential roles of microRNAs and ROS in colorectal cancer: Diagnostic biomarkers and therapeutic targets. Oncotarget 8: 17328-17346, 2017.
32. Lan J, Huang Z, Han J, Shao J and Huang C: Redox regulation of microRNAs in cancer. Cancer Lett 418: 250-259, 2018.
33. Liu Y, Qiang W, Xu X, Dong R, Karst AM, Liu Z, Kong B, Drapkin RI and Wei JJ: Role of miR-182 in response to oxidative stress in the cell fate of human fallopian tube epithelial cells. Oncotarget 6: 38983-38998, 2015.
34. Lv G, Shao S, Dong H, Bian X, Yang X and Dong S: MicroRNA-214 protects cardiac myocytes against H2O2-induced injury. J Cell Biochem 115: 93-101, 2014.
35. Qin SB, Peng DY, Lu JM and Ke ZP: MiR-182-5p inhibited oxidative stress and apoptosis triggered by oxidized low-density lipoprotein via targeting toll-like receptor 4. J Cell Physiol 233: 6630-6637, 2018.
36. Li J, Li J, Wei T and Li J: Down-regulation of MicroRNA-137 improves high glucose-induced oxidative stress injury in human umbilical vein endothelial cells by up-regulation of AMPKα1. Cell Physiol Biochem 39: 847-859, 2016.
37. Shi YF, Liu N, Li YX, Song CL, Song XJ, Zhao Z and Liu B: Insulin protects H9c2 rat cardiomyoblast cells against hydrogen peroxide-induced injury through upregulation of microRNA-210. Free Radic Res 49: 1147-1155, 2015.
38. Li X, Kong M, Jiang D, Qian J, Duan Q and Dong A: MicroRNA-150 aggravates H2O2-induced cardiac myocyte injury by down-regulating c-myb gene. Acta Biochim Biophys Sin (Shanghai) 45: 734-741, 2013.
39. Li QC, Xu H, Wang X, Wang T and Wu J: miR-34a increases cisplatin sensitivity of osteosarcoma cells in vitro through up-regulation of c-Myc and Bim signal. Cancer Biomark 21: 135-144, 2017.
40. Lomonosova E and Chinnadurai G: BH3-only proteins in apoptosis and beyond: An overview. Oncogene 27 (Suppl 1): S2-S19, 2008.
41. Quinsay MN, Lee Y, Rikka S, Sayen MR, Molkentin JD, Gottlieb RA and Gustafsson AB: Bnip3 mediates permeabilization of mitochondria and release of cytochrome c via a novel mechanism. J Mol Cell Cardiol 48: 1146-1156, 2010.
42. Circu ML and Aw TY: Reactive oxygen species, cellular redox systems, and apoptosis. Free Radic Biol Med 48: 749-762, 2010.
43. Cai X, Chen Z, Pan X, Xia L, Chen P, Yang Y, Hu H, Zhang J, Li K, Ge J, *et al*: Inhibition of angiogenesis, fibrosis and thrombosis by tetramethylpyrazine: Mechanisms contributing to the SDF-1/CXCR4 axis. PLoS One 9: e88176, 2014.
44. Yang Z, Zhang Q, Ge J and Tan Z: Protective effects of tetramethylpyrazine on rat retinal cell cultures. Neurochem Int 52: 1176-1187, 2008.
45. Fu YS, Lin YY, Chou SC, Tsai TH, Kao LS, Hsu SY, Cheng FC, Shih YH, Cheng H, Fu YY and Wang JY: Tetramethylpyrazine inhibits activities of glioma cells and glutamate neuro-excitotoxicity: Potential therapeutic application for treatment of gliomas. Neuro Oncol 10: 139-152, 2008.
46. Wang K, Zhu X, Zhang K, Zhou F and Zhu L: Neuroprotective effect of tetramethylpyrazine against all-trans-retinal toxicity in the differentiated Y-79 cells via upregulation of IRBP expression. Exp Cell Res 359: 120-128, 2017.
47. Yu N, Zhang Z, Chen P, Zhong Y, Cai X, Hu H, Yang Y, Zhang J, Li K, Ge J, *et al*: Tetramethylpyrazine (TMP), an active ingredient of chinese herb medicine chuanxiong, attenuates the degeneration of trabecular meshwork through SDF-1/CXCR4 axis. PLoS One 10: e0133055, 2015.
48. Izzotti A, Sacca SC, Cartiglia C and De Flora S: Oxidative deoxyribonucleic acid damage in the eyes of glaucoma patients. Am J Med 114: 638-646, 2003.
49. Zhou B, Li C, Qi W, Zhang Y, Zhang F, Wu JX, Hu YN, Wu DM, Liu Y, Yan TT, *et al*: Downregulation of miR-181a upregulates sirtuin-1 (SIRT1) and improves hepatic insulin sensitivity. Diabetologia 55: 2032-2043, 2012.
50. Muratsu-Ikeda S, Nangaku M, Ikeda Y, Tanaka T, Wada T and Inagi R: Downregulation of miR-205 modulates cell susceptibility to oxidative and endoplasmic reticulum stresses in renal tubular cells. PLoS One 7: e41462, 2012.
51. Lee S, Yun I, Ham O, Lee SY, Lee CY, Park JH, Lee J, Seo HH, Choi E and Hwang KC: Suppression of miR-181a attenuates H2O2-induced death of mesenchymal stem cells by maintaining hexokinase II expression. Biol Res 48: 45, 2015.
52. Cao MQ, You AB, Zhu XD, Zhang W, Zhang YY, Zhang SZ, Zhang KW, Cai H, Shi WK, Li XL, *et al*: miR-182-5p promotes hepatocellular carcinoma progression by repressing FOXO3a. J Hematol Oncol 11: 12, 2018.
53. Wang D, Lu G, Shao Y and Xu D: MiR-182 promotes prostate cancer progression through activating Wnt/β-catenin signal pathway. Biomed Pharmacother 99: 334-339, 2018.
54. Crow MT: Hypoxia, BNip3 proteins, and the mitochondrial death pathway in cardiomyocytes. Circ Res 91: 183-185, 2002.
55. Regula KM, Ens K and Kirshenbaum LA: Inducible expression of BNIP3 provokes mitochondrial defects and hypoxia-mediated cell death of ventricular myocytes. Circ Res 91: 226-231, 2002.
56. Zhang J, Ye J, Altafaj A, Cardona M, Bahi N, Llovera M, Cañas X, Cook SA, Comella JX and Sanchis D: EndoG links Bnip3-induced mitochondrial damage and caspase-independent DNA fragmentation in ischemic cardiomyocytes. PLoS One 6: e17998, 2011.